remote sensing

MDPI

Technical Note

Rapid and Accurate Monitoring of Intertidal Oyster Reef Habitat Using Unoccupied Aircraft Systems and Structure from Motion

Anna E. Windle *,†, Sarah K. Poulin, David W. Johnston and Justin T. Ridge

Division of Marine Science and Conservation, Nicholas School of the Environment, Duke University Marine Laboratory, 135 Duke Marine Lab Rd, Beaufort, NC 28516, USA; skpoulin12@gmail.com (S.K.P.); david.johnston@duke.edu (D.W.J.); justin.ridge@duke.edu (J.T.R.)

* Correspondence: awindle110@gmail.com

† Present address: Horn Point Laboratory, University of Maryland Center for Environmental Science, 2020 Horns Point Rd, Cambridge, MD 21613, USA.

Received: 9 September 2019; Accepted: 12 October 2019; Published: 16 October 2019

Abstract: Oysters support an economically important fishery in many locations in the United States and provide benefits to the surrounding environment by filtering water, providing habitat for fish, and stabilizing shorelines. Changes in oyster reef health reflect variations in factors such as recreational and commercial harvests, predation, disease, storms, and broader anthropogenic influences, such as climate change. Consistent measurements of reef area and morphology can help effectively monitor oyster habitat across locations. However, traditional approaches to acquiring these data are time-consuming and can be costly. Unoccupied aircraft systems (UAS) present a rapid and reliable method for assessing oyster habitat that may overcome these limitations, although little information on the accuracy of platforms and processing techniques is available. In the present study, oyster reefs ranging in size from 30 m^2 to 300 m^2 were surveyed using both fixed-wing and multirotor UAS and compared with ground-based surveys of each reef conducted with a real-time kinematic global positioning system (RTK-GPS). Survey images from UAS were processed using structure from motion (SfM) stereo photogrammetry techniques, with and without the use of ground control point (GCP) correction, to create reef-scale measures of area and morphology for comparison to ground-based measures. UAS-based estimates of both reef area and morphology were consistently lower than ground-based estimates, and the results of matched pairs analyses revealed that differences in reef area did not vary significantly by aircraft or the use of GCPs. However, the use of GCPs increased the accuracy of UAS-based reef morphology measurements, particularly in areas with the presence of water and/or homogeneous spectral characteristics. Our results indicate that both fixed-wing and multirotor UAS can be used to accurately monitor intertidal oyster reefs over time and that proper ground control techniques will improve measurements of reef morphology. These non-destructive methods help modernize oyster habitat monitoring by providing useful and accurate knowledge about the structure and health of oyster reefs ecosystems.

Keywords: *Crassostrea virginica*; eastern oyster; monitoring; unoccupied aircraft systems; remote sensing; reefs; intertidal; structure from motion (SfM)

1. Introduction

Eastern oyster (*Crassostrea virginica)* reefs are important components of coastal and estuarine systems along the Atlantic coast of the United States. Through the long-term consolidation of densely clustered oysters, these reefs provide three-dimensional and complex structures that are fundamental to many coastal ecosystems due to their ability to provide a suite of benefits to the surrounding environment [1–6]. Despite the importance of healthy oyster reefs to coastal ecosystems, it has been estimated that oyster habitat has declined by as much as 85% globally and that many of the remaining populations are in poor condition [6,7]. In the United States alone, a 63% decline in the spatial extent of oyster habitat has been estimated over the past 100 years, with the greatest declines happening along Atlantic coast estuarine systems [8]. Many factors worldwide impact oyster reef health, including overharvesting, predation, diseases, freshwater diversions, non-native species, pollution, habitat degradation, and potentially climate change [9–12].

Guidelines for extensive oyster reef monitoring techniques have been developed for both intertidal and subtidal oyster reef systems to allow for more consistent assessments across varying geographic scales [8,13–16]. Accurate oyster reef dimensions are important for estimations of the total reef area, health and persistence, population abundance, and overall quantity of ecosystem services provided by the oyster reef system to the surrounding environment [2,8,17,18]. Specifically, monitoring metrics, such as oyster reef area and morphology, have been noted as key indicators for oyster reef health and growth [19–24]. Reef morphology refers to the structural complexities of an intertidal oyster reef, including elevation and rugosity.

Intertidal oyster reefs are typically monitored when exposed to the air at low tide, and, for decades, intertidal oyster reefs have been mapped using a combination of global positioning system (GPS) and geographical information systems (GIS) [24,25]. GPS units can collect continuous coordinate points of a reef to obtain area, height, and morphological measurements [13,19,23,26,27]. These traditional intertidal oyster reef monitoring methods can be time and labor-intensive, damaging to the reef environment, and subject to human inconsistencies. These traditional methods can also limit the ability of management to monitor large areas of intertidal oyster habitat, as reef mapping may only occur every 10 to 15 years, making monitoring of intertidal reef health, change, and restoration difficult [28,29].

In recent years, additional remote sensing techniques have been developed to more effectively monitor oyster reef habitat [29,30]. Researchers and managers have used aerial imagery from occupied aircraft to assess long term changes in spectral characteristics, detect environmental and anthropogenic stressors in oyster reef distribution, and measure loss over time [24,31–33]. Satellite remote sensing has also been used to distinguish shellfish substrates from bare sediment, allowing for mapping of intertidal oyster habitat [29,30,34,35]. These traditional remote sensing methods allow for manual delineation, which can approximate the size of oyster reefs in many cases; however, temporal lags in image acquisition and low resolution from aircraft and satellites can miss rapid changes in finer-scale or slightly submerged patches of oysters (Figure 1) [28,34]. Studies have shown that historical aerial imagery represents a crude estimation of intertidal oyster habitat, failing to reliably assess oyster habitat loss [28]. Terrestrial and aerial light detection and ranging (LiDAR) have been used to assess the vertical height, elevation, and morphology of intertidal reefs as well as distinguish between mud, bleached dead shell, and live shell by measuring differing vertical clusters with return intensity [23,29]. Additionally, intertidal oyster reef elevations are critical for understanding reef morphology change as well as specific placement within the tidal range [21,22]. However, the cost at an adequate vertical resolution has generally been too great to implement on a broad scale. These remote sensing methods can be more efficient than direct monitoring methods. However, they can still be time-intensive, expensive, and limit the ability to collect information for large regional areas.

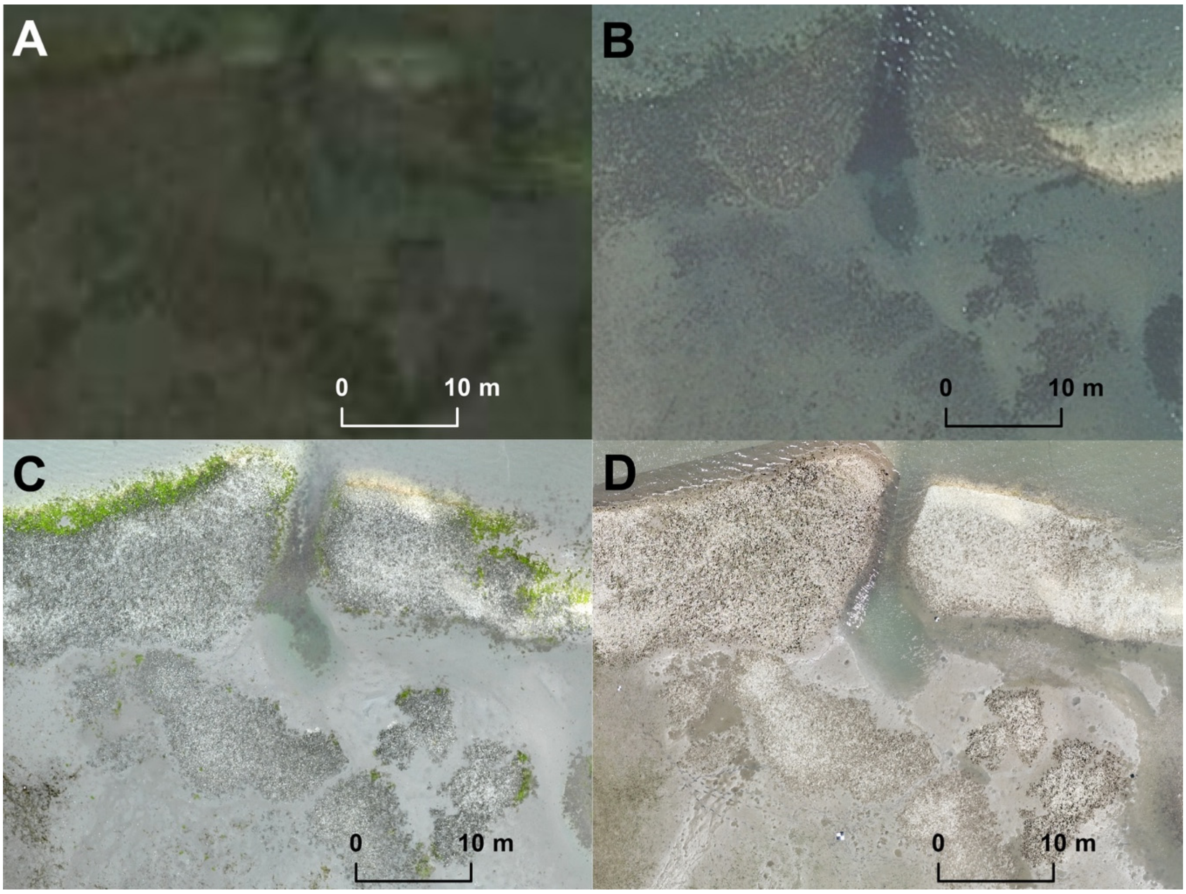

Figure 1. Comparison of imagery used to assess intertidal oyster reefs with the same scale and extent on Town Marsh, Rachel Carson Reserve, part of the North Carolina National Estuarine Research Reserve (NCNERR), Beaufort, NC. (**A**) Google Earth imagery, as used by Grizzle et al. (2018) [26]. (**B**) 0.15 × 0.15 m high-resolution orthoimagery taken February 2012 and accessed from United States Geological Survey (USGS) Earth Resources Observation and Science (EROS) Archive. (**C**) 0.02 × 0.02 m resolution unoccupied aircraft systems (UAS) imagery from an eBee fixed-wing flight taken in March 2018. (**D**) 0.006 × 0.006 m resolution UAS imagery from a DJI Mavic Pro multicopter flight taken in May 2018.

Remote sensing via unoccupied aircraft systems (UAS, or drones), is an emerging method to collect coastal data [36–39]. Fixed-wing and multirotor UAS can conduct aerial surveys to map natural and restored intertidal oyster reefs. UAS imagery is stitched together using a photogrammetric imaging technique, structure from motion (SfM), which produces orthomosaics and three-dimensional digital surface models from two-dimensional image sequences at centimeter resolution. SfM methods have been used for fine-scale 3D mapping of coastal areas, with comparable results to terrestrial laser scanning surveys [40,41]. UAS remote sensing has the potential to be a low cost, rapid, and accurate method for assessing intertidal oyster habitat allowing for replicability over time. The present study compares intertidal oyster reef area and morphology measurements generated through the use of SfM photogrammetry techniques using UAS imaging. The results of this comparison can be used by coastal managers, practitioners, and scientists to help guide and expedite efforts to accurately monitor and assess natural and restored oyster reefs over time.

2. Methods

2.1. Study Area

The Rachel Carson Reserve (part of the North Carolina National Estuarine Research Reserve) is located adjacent to the town of Beaufort in Carteret County, NC, USA. The Rachel Carson Reserve consists of fetch-limited barrier islands (Town Marsh, Bird Shoal, and Carrot Island) and a saltmarsh island complex (Middle Marsh). Semidiurnal tides with a 0.9 m tidal range contribute to extensive saltmarsh platforms, intertidal oyster reefs, shallow seagrass beds, and tidal flats across the low-lying landscape. UAS flights were conducted over natural fringing and restored intertidal oyster reefs within the Reserve (Figure 2). An oyster reef consisted of an aggregation of oysters that were observably distinguishable to the surrounding environment, and the percent cover of shell had to exceed 25%. This coverage was chosen to allow us to separate sparse clustering from consolidating reef aggregations. Reefs within this region can exist from just below mean low water (MLW; −0.42 m North American Vertical Datum of 1988 (NAVD88)) to just above mean sea level (MSL; ~0.0 m NAVD88) [22–24]. Natural intertidal fringing and isolated reefs at Town Marsh are located along the shoreline of the island adjacent to salt marsh and maritime forest. Intertidal reefs at Town Marsh are well developed, and harvesting is prohibited. Restored intertidal patch reefs located in Middle Marsh are isolated reefs, constructed in 1997 and 2000 (3 m × 5 m footprints) [14], located on a sandflat that is only fully exposed during spring tides. Harvesting is allowed within Middle Marsh with the season occurring from October to March.

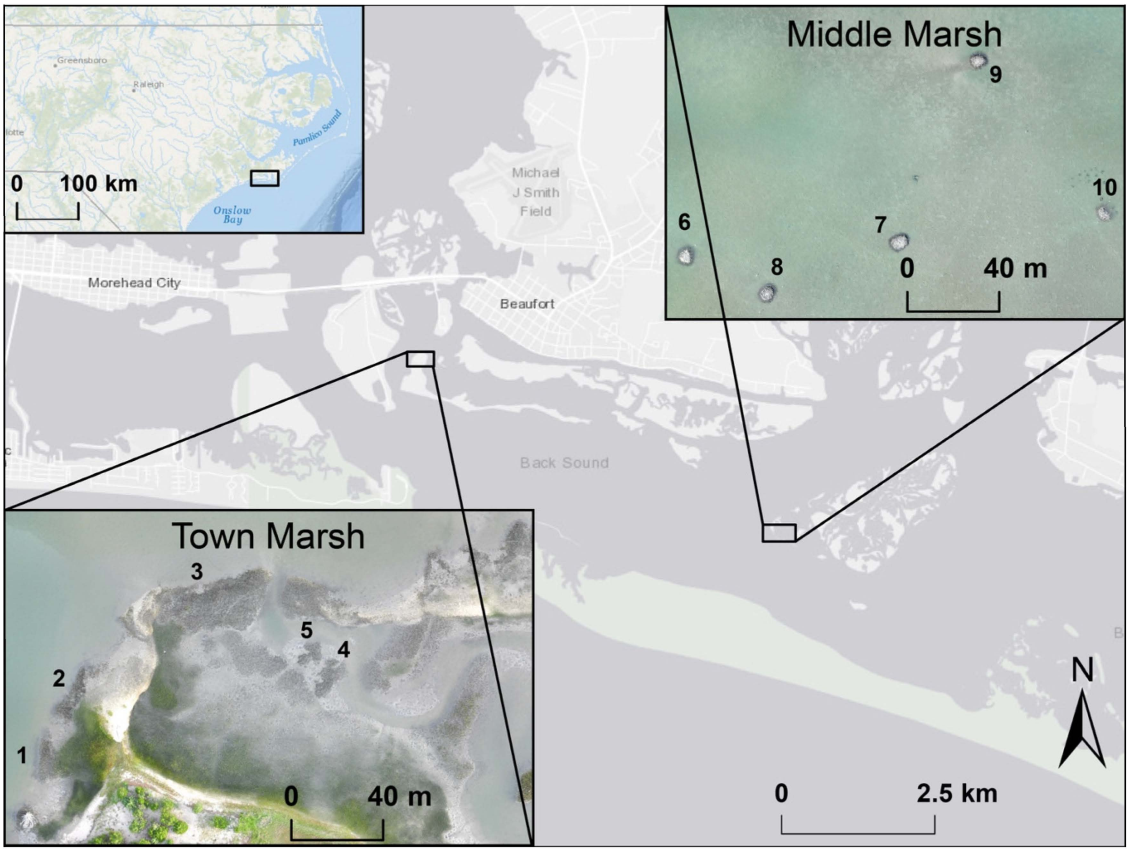

Figure 2. Study area of Town Marsh and Middle Marsh located within the Rachel Carson Reserve, part of the North Carolina National Estuarine Research Reserve (NCNERR, Beaufort, N.C.). Insets include fringing intertidal oyster reefs at Town Marsh and restored intertidal patch reefs at Middle Marsh taken from the senseFly eBee UAS.

2.2. Traditional Field Surveys

Five natural fringing reefs were chosen for measurements at Town Marsh, and five restored patch reefs were chosen for measurements at Middle Marsh. Reefs at Town Marsh were chosen for their proximity to each other in the UAS flight extent. A real-time kinematic (RTK) GPS uses base station corrections to achieve 3 cm-level accuracy. To calculate reef area, an RTK GPS (Reach RS, Emlid, Hong Kong) was used to make continuous measurements (1 m increments) while walking along the perimeter of a reef during low tide. Coordinates were imported into ArcMap mapping software version 10.5 (ESRI Inc., Redlands, CA, USA) to calculate the area of plotted reefs in m^2 (Figure 3). To capture the elevation profile of each reef, RTK GPS elevations were also taken every meter along the crest of a reef, which was considered an approximate centerline of the long axis of the reef that contained a range of elevation measurements.

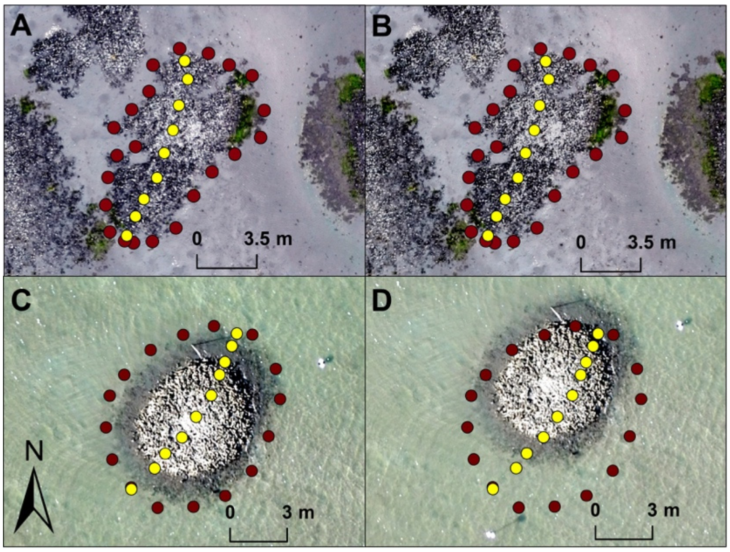

Figure 3. Comparison of oyster reef location between sites and the use of ground control points (GCPs) to correct horizontal accuracy of UAS imagery. (**A**) A fixed-wing eBee flight over Town Marsh reefs processed with GCPs and (**B**) without GCPs. (**C**) An eBee flight over Middle Marsh reefs processed with GCPs and (**D**) without GCPs. RTK-GPS measurements of the reef crest (yellow points) and perimeter (red points) are included for location reference.

2.3. Unoccupied Aircraft Systems

Two different aircraft were deployed as part of these surveys, including fixed-wing and multirotor aircraft. The fixed-wing aircraft (senseFly eBee Plus) and multirotor aircraft (DJI Mavic Pro) collected data in spring 2018. The eBee was equipped with a senseFly Sensor Optimized for Drone Applications (S.O.D.A.) 20-megapixel RGB camera, and a survey-grade RTK GPS capable of 3 cm of horizontal error, allowing for more accurate image geotags. The survey altitude of approximately 57 m corresponded to a ground sampling distance (GSD) of 0.022 m and imagery was collected off-nadir at a 5 to 7° pitch angle due to how the UAS reduces motor vibration during photo collection. This slight off-nadir imagery does not impact final products, as camera position is incorporated into the structure from motion process. All flights were automated, with flight plans and image transects generated and executed in the eMotion 3 ground control software programs with 75% to 85% longitudinal and 75% lateral image overlap.

The DJI Mavic Pro quadcopter was equipped with a 12.35-megapixel RGB camera. Flights were completed through a combination of automated and manual flight plans. Image transects were generated and executed in the Pix4D Capture software program with a 71% to 75% overlap. The camera angle was set off-nadir at a 10 to 15° pitch angle with a flight altitude of approximately 50 m, resulting in a GSD of 0.0058 m. All UAS operations occurred within the Federal Aviation Administration (FAA) Part 107 guidelines.

Ground control points (GCPs), typically black and white 'checker' targets with defined center points, were used to help increase geolocation accuracy of UAS imagery, which can also help during the structure from motion photogrammetry process. Before each flight, the center of 4 to 10 GCPs was surveyed using an RTK GPS. Each flight's imagery was processed twice, once with the registration of GCPs and once without, to assess the necessity for GCPs in achieving desirable reef measurements. All UAS imagery was processed with Pix4D Mapper Pro photogrammetry software (version 4.2.27, Switzerland) to output RGB orthomosaics and digital surface models (DSMs) in the WGS1984 UTM Zone 18N projection. The DSMs were created using an inverse distance weighting method, allowing for surface smoothing at 1.12 to 2.21 cm/pixel. For DSMs generated by the RTK-equipped eBee and the GCP-registered Mavic Pro flights, surface model heights were converted to elevations in the North American Vertical Datum of 1988 to create a digital elevation model (DEM). Therefore, only the Mavic flights without GCP registrations remained as a DSM.

2.4. Remote Sensing Evaluation Methods

Reef area and elevation remote sensing measurements were conducted on orthomosaics and DEMs generated from both UAS types with and without the use of GCPs. To determine reef area, individual reefs from the orthomosaics from both aircraft at each site were manually delineated in ArcMap to create a layer for each reef. From the eBee flights, five fringing reefs were chosen for measurements at Town Marsh and Middle Marsh, while the Mavic flights included five fringing reefs from Town Marsh and three patch reefs from Middle Marsh due to a smaller flight extent. Reef layers were then vectorized to produce polygon feature classes with measurable values of area (m^2). UAS-derived reef areas were then subtracted from GPS-obtained reef areas to compare the difference of UAS-derived areas to standard GPS point collection. Root mean square error (RMSE) was calculated for each difference between UAS and GPS-derived areas.

To collect reef morphological information, the same reefs delineated for reef area were examined, and UAS-derived elevation values from each DSM/DEM were extracted at GPS coordinates along the reef crest. UAS reef elevations were then subtracted from the GPS-obtained reef elevations, and data were analyzed by aircraft type and GCP correction to compare the accuracy of UAS derived DSM/DEM elevations to standard RTK GPS point collection, which we consider to be the true values. When uncorrected (non-GCP registered) imagery was misaligned from the true position (Figure 3), manual points were created to extract elevation data of the reefs. Root mean square error (RMSE) was calculated for each difference between UAS and GPS-derived elevations.

2.5. Statistical Analysis

Comparisons of UAS and GPS-derived measurements were analyzed across and within sites, by aircraft, and whether imagery was corrected and uncorrected with GCPs. To control for varying conditions between sites, metrics were analyzed separately on reefs located in Town Marsh and Middle Marsh. All statistical tests were run on R (version 3.5.1) and Rstudio (version 1.1.383) [42]. Normally distributed data allows for the use of parametric statistical tests. The assumption of normality of the reef area differences and elevation data was assessed using Shapiro–Wilk normality tests, and Chi-squared tests detected outliers.

When all intertidal oyster reef area differences were analyzed with both sites combined, all data were normal with no outliers ($n = 10$ eBee, $n = 8$ Mavic). When reef area differences were separated by site, all data were considered normal ($n = 5$ eBee, $n = 5$ Mavic). All reef area differences at Middle Marsh were also considered normal and contained no outliers ($n = 5$ eBee, $n = 3$ Mavic). A series of matched paired *t*-tests were used to compare mean differences between the paired values of GPS and UAS-derived area measurements of the same oyster reefs.

When reef elevation measurements at both sites were analyzed together, the removal of an outlier could not satisfy normality. Therefore, a series of nonparametric matched Wilcoxon tests were used to compare mean elevation differences between paired values of GPS and UAS-derived elevation measurements of the same oyster reefs (n = 10 eBee, n = 8 Mavic). Matched Wilcoxon tests were also used to analyze reef elevation measurements when separated by site, (n = 5 eBee and Mavic for Town Marsh, n = 5 eBee and n = 3 Mavic for Middle Marsh).

3. Results

3.1. Initial Processing and GCP Correction

Visual examination of the resulting orthomosaics indicated that the GPS points lined up well on both GCP corrected and uncorrected imagery from Town Marsh and on the corrected imagery at Middle Marsh, but the uncorrected imagery from Middle Marsh resulted in misalignment from the true position (Figure 3). This was potentially due to the number of key points (unique pixel clusters) that were available for the SfM processing. Imagery from both aircraft over Town Marsh contained between 5000 and 12,000 2D matched key points while imagery from both aircraft over Middle Marsh generated an average of 2234 2D key points.

3.2. Reef Area

UAS-derived reef area measurements differed from GPS-derived area measurements depending on aircraft and site. Detailed area measurements and comparisons are described in Table 1. Processing with and without GCPs did not significantly influence UAS-derived reef area measurements (Figure 4); therefore, the following data are from the GCP-corrected flights. When all reef at both sites were analyzed, matched paired analyses revealed that both eBee and Mavic corrected UAS-derived reef area measurements were significantly different than GPS-derived reef area measurements with UAS-derived measurements typically being smaller in area than the GPS-derived measurements (Table S1, Figure 5). When reefs were analyzed separately at each site, matched pair analyses revealed that corrected UAS-derived area measurements were not significantly different than GPS-derived measurements in Town Marsh. Matched pair analyses also revealed that corrected UAS-derived area measurements were only significantly different than GPS-derived measurements in the eBee imagery (Table S1).

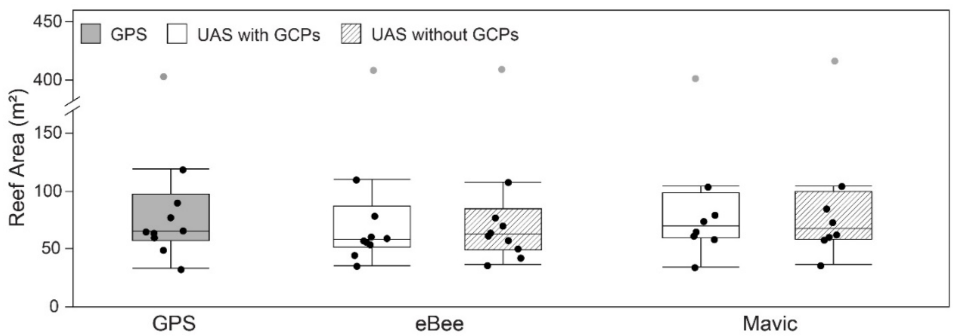

Figure 4. Reef areas calculated from a real-time kinematic (RTK) global positioning system (GPS) perimeter and two UAS (senseFly eBee fixed-wing and DJI Mavic Pro quadcopter) that were processed with and without ground control point (GCP) correction.

Table 1. Global positioning system (GPS) and unoccupied aircraft system (UAS)-derived intertidal oyster reef area measurements in m^2 from five reefs located in Town Marsh and Middle Marsh. Only three intertidal reef area measurements are included in the Mavic flights at Middle Marsh due to a small flight extent. Percentage of reef area differences are shown in parentheses.

Reef	GPS	eBee		Mavic	
	Area	Area	ΔGPS-eBee	Area	ΔGPS-Mavic
	Town Marsh (m^2)				
1	90.57	79.15	11.42 (12.61%)	80.00	10.57 (11.67%)
2	119.33	110.55	8.78 (7.36%)	104.38	14.95 (12.53%)
3	402.41	407.87	5.46 (1.36%)	400.78	1.64 (0.41%)
4	64.39	57.746	6.64 (10.32%)	58.94	5.45 (8.46%)
5	33.03	35.85	2.82 (8.54%)	34.69	1.66 (5.03%)
Average ± S.D.			7.02 ± 3.27		6.85 ± 5.82
RMSE			7.61		8.61
	Middle Marsh (m^2)				
6	77.92	61.19	16.73 (21.47%)	74.54	3.38 (4.34%)
7	66.47	59.85	6.62 (9.96%)	65.42	1.05 (1.58%)
8	65.51	56.65	8.86 (13.52%)	61.88	3.63 (5.54%)
9	60.46	54.47	5.99 (9.91%)	NA	NA
10	49.64	45.23	4.41 (8.88%)	NA	NA
Average ± S.D.			6.47 ± 1.85		2.69 ± 1.83
RMSE			9.57		2.93

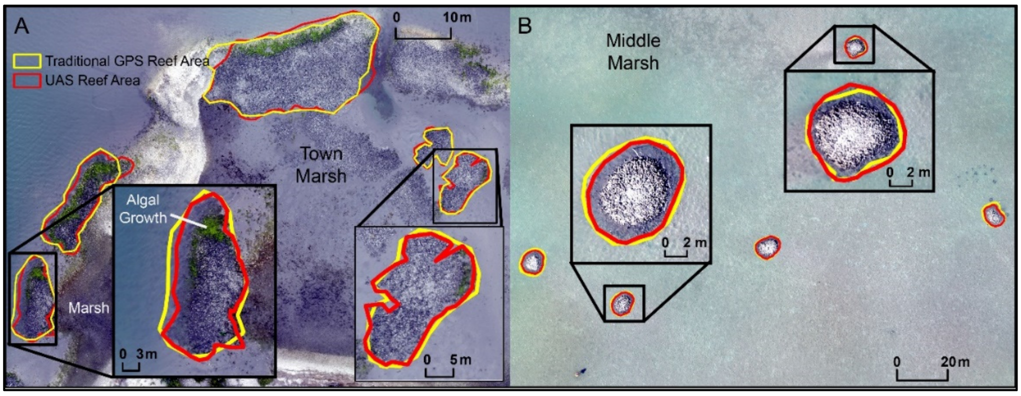

Figure 5. Intertidal oyster reef boundaries from eBee fixed-wing UAS imagery (red) and RTK GPS derived polygons (yellow) of fringing oyster reefs located in Town Marsh (**A**) and restored patch reefs in Middle Marsh (**B**) Rachel Carson Reserve, Beaufort, NC.

3.3. *Reef Morphology*

UAS-derived reef elevation measurements differed from GPS-derived elevation measurements depending on aircraft and site. Reef elevation measurements were also compared using GCP-registered (corrected) and non-GCP-registered (uncorrected) imagery; however, elevations generated when Mavic Pro imagery was processed without GCP corrections proved too inconsistent, with altitude estimates deviating on the order of 10 m, and were, therefore, excluded. Elevation measurements are all described in Table 2, together with the absolute difference and RMSE of each method from the GPS elevations. When all intertidal oyster reefs from both sites were compared, nonparametric matched paired analyses revealed significant differences in GPS and UAS-derived mean reef elevations in the corrected eBee imagery (Table S2). There were no significant differences in GPS and UAS-derived mean reef elevations when elevations were compared at separate sites (Table S2); however, several approached significance.

Table 2. GPS and UAS-derived intertidal average oyster reef elevation measurements in meters (NAVD88) from five reefs located in Town Marsh and Middle Marsh from a corrected eBee and uncorrected with GCPs and a Mavic Pro corrected with GCPs. Only three intertidal reef area measurements are included in the Mavic flights at Middle Marsh due to a small flight extent.

		eBee				Mavic	
Reef #	**GPS**	**Corrected**	**Uncorrected**	**ΔGPS-Corrected**	**ΔGPS-Uncorrected**	**Corrected**	**ΔGPS-Corrected**
Town Marsh (m)							
1	−0.23	−0.18	−0.16	0.05	0.07	−0.23	0.02
2	−0.17	−0.12	−0.11	0.05	0.07	−0.18	0.02
3	−0.11	−0.08	−0.06	0.03	0.05	−0.13	0.03
4	−0.20	−0.13	−0.11	0.04	0.05	−0.18	0.01
5	−0.17	−0.17	−0.21	0.05	0.05	−0.24	0.04
Average ± S.D.				0.04 ± 0.01	0.06 ± 0.01		0.02 ± 0.01
RMSE				0.05	0.06		0.03
Middle Marsh (m)							
6	−0.30	−0.28	−1.26	−0.41	0.06	0.62	0.09
7	−0.19	−0.16	−1.16	−0.54	0.05	0.97	0.35
8	−0.20	−0.15	−0.85	−0.03	0.05	0.65	0.17
9	−0.23	−0.16	−0.42	NA	0.07	0.24	NA
10	−0.18	−0.13	−1.37	NA	0.05	1.19	NA
Average ± S.D.				0.06 ± 0.01	0.73 ± 0.36		0.20 ± 0.13
RMSE				0.05	0.86		0.23

In general, UAS-derived reef elevations showed higher differences to GPS-derived elevations along reef edges (Figure 6). Point-by-point comparisons of the corrected Mavic and GPS elevations showed the highest differences on Town Marsh reef edges and slightly higher differences on all Middle Marsh reefs. The uncorrected eBee imagery showed the highest elevation differences along reef edges at both sites and more overall elevation differences in Middle Marsh. The corrected eBee imagery had improved elevation differences at both sites (Figure 6).

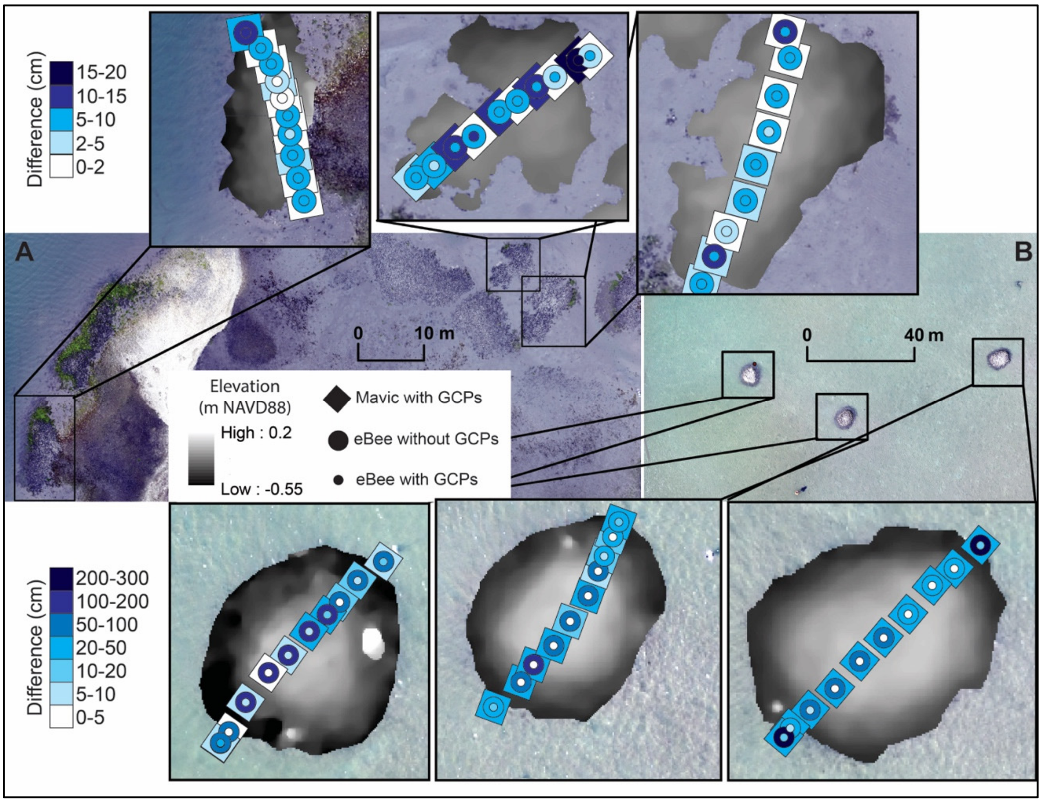

Figure 6. eBee UAS derived DEMs clipped to fringing intertidal oyster reefs in Town Marsh (**A**) and restored intertidal patch reefs Middle Marsh (**B**) with direct comparisons between RTK-GPS elevations

and UAS-derived elevations extracted from each point for DEMs created from the GCP-registered Mavic (diamonds), eBee without GCP registration (large circles), and GCP-registered eBee (small circles). Deviations are colored by their absolute difference from the GPS points; note different scales between Town Marsh and Middle Marsh reefs.

4. Discussion

4.1. Reef Area

Delineating intertidal oyster reefs by analyzing high-resolution UAS orthomosaics proved to be an effective and quick method to calculate reef area (Figure 5). The nature of delineating reef edges from aerial imagery allows for greater point generation with minimal increase in effort and likely increases reef edge fidelity. Site seemed to influence the area measurements between UAS and GPS-derived methods. When all patches from both sites were combined, there were significant differences between the two methods (Table S1). However, when observing differences from each site independently, significant relationships changed. At Town Marsh, there were no significant differences in reef area between UAS and GPS methods (Table S1), indicating that UAS methods have the potential to provide similar area measurements to traditional GPS methods on natural intertidal oyster reefs. However, when UAS and GPS methods were compared from Middle Marsh, there were significant differences in reef area from the eBee flight (Table S1). The eBee flight over Middle Marsh occurred when the restored reefs were partially inundated, which could have contributed to differences in measurements of area. The small scale oyster reefs analyzed in this study may be poorly defined in occupied aerial and satellite imagery depending on conditions (Figure 1) and could, therefore, be excluded from population estimates derived from these lower resolution images. The small inaccuracies that may occur due to these occlusion effects would still be preferable compared to the absence of small reefs in traditional oyster mapping datasets. The on-demand nature of UAS allows managers to more readily collect high-resolution data optimized for seasonal and tidal conditions.

There are several caveats to delineating reef edges that were observed during this study. Continuous RTK-GPS sampling is recommended for calculating intertidal oyster reef area in the field [13]. However, a backpack GPS attachment is recommended to maintain steady motion and continuous measurements while walking the perimeter of oyster reefs, which was not used in this study. This method likely would have reduced differences between the GPS-derived areas and the UAS-derived areas and should be practiced if available. Differences in area could also be attributable to the subjectivity of users delineating the reef edge when examining an orthomosaic, particularly if the edge is submerged in cloudy water or extending into a vegetated habitat. This was likely minimal on these study reefs, which generally have well-defined edges. Additionally, the boundary of reefs became obscured during high tides due to the mixing of sediment and water, hindering both GPS and UAS-derived reef perimeter measurements. Seasonal changes in oyster reefs, such as algal growth in the spring, could also affect a reef delineation [43,44] (Figure 7). Analyzing UAS imagery without proper knowledge of the oyster landscape could lead to inaccurately classifying oyster habitat due to visual obstruction from algal growth. Seasonal fluctuations in water clarity may provide opportunities to capture rough reef area without the need for a spring low tide, but refraction and wave action may contribute to some visual inaccuracy.

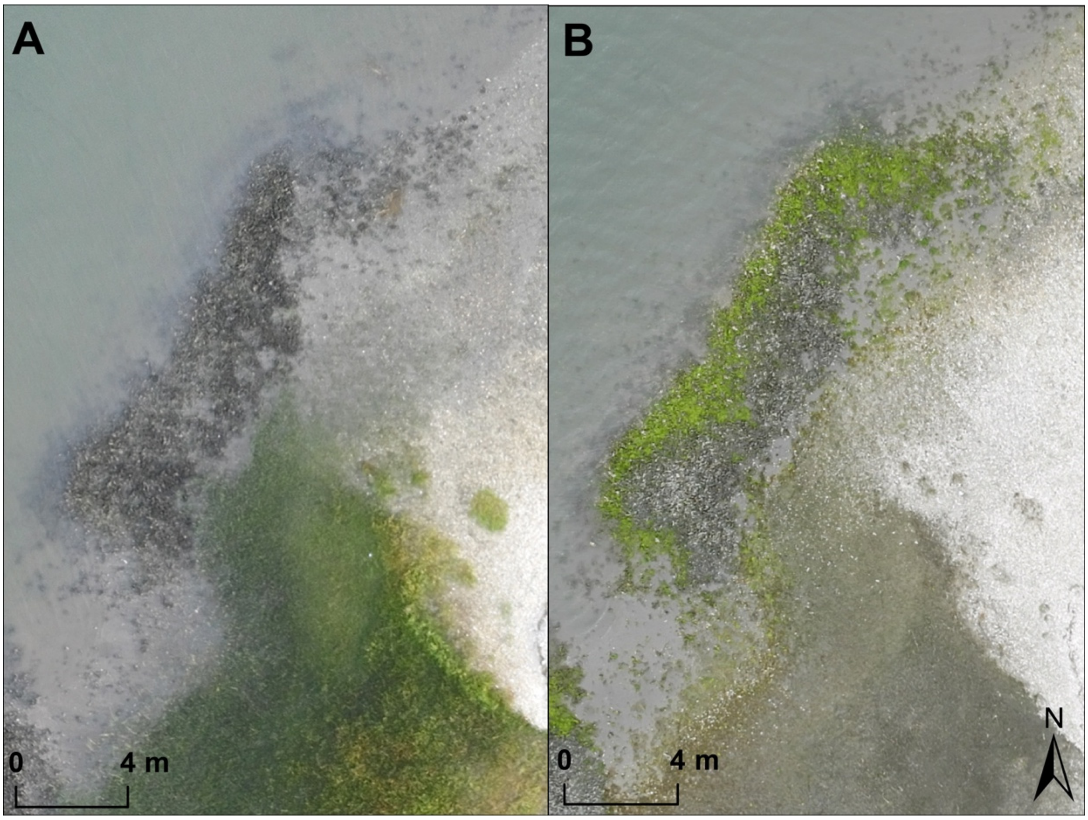

Figure 7. Comparison of an individual fringing oyster reef on Town Marsh, Rachel Carson Reserve, NCNERR between (**A**) Fall 2017 and (**B**) Spring 2018 collected from fixed-wing eBee UAS. Reef area delineation could be impacted by algal growth and inundation level.

4.2. Reef Morphology

In general, average UAS-derived oyster reef elevations were less than the traditional GPS-derived elevations on all reefs, indicating the UAS-derived DSM/DEM could be underestimating the true surface (Table 2). However, most UAS-derived reef elevations were less than 10 cm different than traditional GPS methods with the greatest differences in point-by-point comparisons occurring at the reef edges and particularly in Middle Marsh (Figure 6). With the exception of the corrected eBee and Middle Marsh uncorrected eBee, DEM elevations were not significantly different from GPS elevations, which is most likely due to the variability in measurements (Table S2). However, the overall significance exhibited by the corrected eBee is most likely due to overall lower UAS-derived elevation values with a small standard deviation (higher precision).

The variability of oyster reef morphology differences supports the difficulty SfM software has in recreating DSMs in homogenous textured environments. When plotted, GPS points did not line up well with uncorrected imagery from Middle Marsh (Figure 3). The shift in points is potentially due to the challenge of processing imagery over shallow water [38,45] and the homogenous low contrast texture of the sandflat [41]. More key points (unique pixel clusters) were found in Town Marsh imagery due to the spectrally complex surrounding terrestrial environment compared to Middle Marsh patch reefs that were located on a broad sandflat with minimal spectral texture differences to identify key points. The number of median key points per image for the Middle Marsh flights was generally half the key points generated for Town Marsh. Therefore, the stitched DSM could have been affected by the lack of tie points in Middle Marsh exacerbating reef elevation differences, particularly at the edges of reefs that may have been inundated during some flights (Figure 6). The eBee flight over Middle Marsh was further hindered by the presence of water atop the sandflat as the tide did not drop as low as predicted, making it challenging for the processing software. Conversely, the Mavic flight over the Middle Marsh reefs was conducted on a lower tide with full exposure of the sandflat, which appears to have created a more accurate DSM that better captures the deeper elevations of the reefs and surrounding substrate.

Lastly, observed reef morphology variability could have also been due to disparities in aircraft components between the commercial-grade eBee and the consumer-grade Mavic Pro. The eBee is equipped with a mapping-grade camera that has a much larger sensor than the Mavic Pro and is optimized for taking still imagery while flying, unlike the Mavic Pro camera, which is better suited for video acquisition. Additionally, the eBee is equipped with an advanced GPS to create more accurate image geotags (x,y,z location, and camera angle of images), which makes the photogrammetry process more effective. Depending on the level of accuracy desired, either aircraft may be appropriate when coarse measurements will suffice, but finer measurements may require either a commercial-grade aircraft or the use of GCPs.

4.3. Broader Implications

The combination of UAS technology, SfM software, and GIS offers a variety of useful tools for the management and conservation of many coastal habitats. Digital surface models obtained by SfM methods have been found to have higher resolution than traditional surveying methods, leading to higher precision in extracted features, especially on coastal habitats [46]. In some cases, it can deliver coastal topographic measurements better than existing LiDAR methods and comparable to that of a terrestrial laser scanning solution [40,41,46]. UAS-SfM imagery and topographic data SfM approaches have also been used to measure mangrove forest canopy height and quantify underwater coral reefs [47,48]. High resolution, on-demand imaging of oyster habitats, can provide an efficient method to calculate reef area, a more holistic measurement of reef morphology, and the ability to quickly measure vertical changes to the reef from growth or anthropogenic impacts without damaging adjacent habitats. In addition, UAS methods have the potential to increase the efficiency of oyster reef monitoring exponentially as reef extent increases. Replicability of this analysis at other locations is possible when using UAS imagery taken at a low tide when turbidity and wave height do not impact intertidal oyster reef visibility. Additionally, some sites may require oblique UAS flights due to the canopy cover and shadow of adjacent vegetation [43].

In general, it is good practice to use GCPs to ensure data are the most accurate. RTK-equipped aircraft may reduce reliance on GCPs, as evidenced by our results in Town Marsh with the eBee. Without the added time for GCP deployment, a UAS can collect data from ~25 acres in 20 min, which is substantially quicker than collecting data of that extent in the field. However, the reef morphology comparison from this study indicates using GCPs can increase the accuracy of DSM elevation values, especially in areas that are surrounded by water with little terrestrial environment to help process the images together. It should also be noted that the use of GCPs also produces an absolute frame of reference allowing for more direct comparisons with other datasets collected in the same area by different UAS and sensors at different times. Without GCPs, the positional error of the UAS-derived data could be on the order of 10 cm to well over 1 m depending on the type of aircraft used and may provide data products only suitable for relative comparisons. However, some coastal management programs may not require centimeter-level precision to achieve monitoring goals, and the use of GCPs may be superfluous. Furthermore, deployment of GCPs, unless permanent, still requires the need to directly access a site, potentially negating the 'rapid and low disturbance' benefits of UAS. Permanent GCPs within a study area would reduce the time required to survey a site. Overall, these results are promising for the potential future implementation of UAS without the need for GCPs at all locations of interest.

Although the aircraft were of different types, used different sensors, and flew at varying altitudes, they achieved similar results. This speaks to the robustness of SfM at using different quality images to reconstruct three-dimensional environments with relatively good fidelity (~10 cm), and that the aircraft and sensor can be fairly flexible depending on the mission requirements. The Mavic Pro quadcopter is a highly affordable consumer-grade option; however, it cannot fly as long and cover as much area as the fixed-wing eBee. The Mavic can be easily launched from a boat or any dry surface, while the eBee requires a larger dry area free of obstacles to descend and land. Aircraft can be chosen for different scales of management and should be evaluated in terms of area to be covered, type of environment, and affordability. In addition, depending on the type of aircraft and application, UAS methods may present a cheaper alternative to other forms of data collection. It should also be noted that DJI has since released the Mavic 2 with an improved sensor payload, and continued advancements to consumer-grade UAS sensors and GPS technology will further increase the accuracy of results from these aircraft.

5. Conclusions

UAS remote sensing with SfM is a rapidly evolving technology for coastal environments [37] and has the capability to advance the way scientists and managers monitor oyster reefs and other environments. UAS mapping techniques provide a more cost-effective, repeatable, and timely method for producing baseline and time series habitat maps of intertidal oyster reefs. It can enhance traditional in situ field surveys with similar results while reducing the amount of time, energy, and disturbance involved to obtain the same information. Different aircraft may be better suited depending on the scale of monitoring, and site conditions may dictate the need for GCPs and the expected accuracy of the resulting products. The methods described in the present study would allow coastal managers to analyze a large study region relatively quickly to assess the growth, health, or impacts of intertidal oyster reefs with minimal disturbance.

Supplementary Materials: The following are available online at http://www.mdpi.com/2072-4292/11/20/2394/s1, Table S1: Matched paired analyses comparing corrected and uncorrected UAS–derived area differences from both aircraft to traditional GPS–derived reef areas. * denotes p-value < 0.05., Table S2: Wilcoxon matched paired analyses comparing corrected and uncorrected UAS–derived reef elevations from both aircraft to traditional GPS–derived reef elevations. * denotes p-value < 0.05.

Author Contributions: Conceptualization, A.E.W., S.K.P. and J.T.R. Methodology, A.E.W., S.K.P., J.T.R.; Investigation and Formal Analysis, A.E.W., S.K.P. and J.T.R.; Resources, D.W.J.; Data Curation, A.E.W., J.T.R.; Writing—Original Draft Preparation, A.E.W., J.T.R.; Writing—Review and Editing, A.E.W., S.K.P., J.T.R., D.W.J.; Visualization, A.E.W., J.T.R.; Supervision, D.W.J.; Project Administration, J.T.R., D.W.J.; Funding Acquisition, A.E.W., S.K.P., J.T.R.

Funding: We thank the support of both the North Carolina Sea Grant/Space Grant Fellowship program and the North Carolina Division of Marine Fisheries for their support in funding the project. This research was supported by the North Carolina Sea and Space Grant Graduate Fellowship (Grant #2017-R/MG-1710) as well as the North Carolina Coastal Recreational Fishing License Grants Program (Marine Resources Fund, Grant # 2017-H-068).

Acknowledgments: We thank Brandon Puckett, Research Coordinator of the Rachel Carson Reserve (NCNERR), for sharing his knowledge of the reserve and his guidance through the development of the project and also for providing transportation to study sites. We thank Alex Seymour for GIS guidance and constructive feedback throughout the extent of the project and for piloting the fixed-wing UAS flights. We appreciate the time and efforts given by Julian Dale with UAS flight planning and performance in the field. We thank Wendy Folfas, Kelly Dobroski, Claire Atkins-Davis, and Virginia Pan for assisting in fieldwork.

Conflicts of Interest: The authors declare no conflicts of interest.

References

1. Coen, D.L.; Humphries, A. Oyster-generated marine habitats: Their services, enhancement, restoration, and monitoring. In *Routledge Handbook of Ecological and Environmental Restoration*; Murphy, S., Allison, S., Eds.; Taylor & Francis Group/Routledge: Cambridge, UK, 2017; pp. 275–295.
2. Grabowski, J.H.; Brumbaugh, R.D.; Conrad, R.F.; Keeler, A.G.; Opaluch, J.J.; Peterson, C.H.; Piehler, M.F.; Powers, S.P.; Smyth, A.R. Economic valuation of ecosystem services provided by oyster reefs. *BioScience* **2012**, *62*, 900–909. [CrossRef]
3. Kellogg, M.L.; Smyth, A.R.; Luckenbach, M.W.; Carmichael, R.H.; Brown, B.L.; Cornwell, J.C.; Piehler, M.F.; Owens, M.S.; Dalrymple, D.J.; Higgins, C.B. Use of oysters to mitigate eutrophication in coastal waters. *Estuar. Coast. Shelf Sci.* **2014**, *151*, 156–168. [CrossRef]

4. McLeod, I.M.; zu Ermgassen, P.S.; Gillies, C.L.; Hancock, B.; Humphries, A. Can Bivalve Habitat Restoration Improve Degraded Estuaries? In *Coasts and Estuaries*; Elsevier: Amsterdam, The Netherlands, 2019; pp. 427–442.
5. Smaal, A.C.; Ferreira, J.G.; Grant, J.; Petersen, J.K.; Strand, Ø. (Eds.) *Goods and Services of Marine Bivalves*; Springer: Berlin/Heidelberg, Germany, 2018.
6. Ysebaert, T.; Walles, B.; Haner, J.; Hancock, B. Habitat modification and coastal protection by ecosystem-engineering reef-building bivalves. In *Goods and Services of Marine Bivalves*; Springer: Berlin/Heidelberg, Germany, 2019; pp. 253–273.
7. Kirby, M.X. Fishing down the coast: historical expansion and collapse of oyster fisheries along continental margins. *Proc. Natl. Acad. Sci. USA* **2004**, *101*, 13096–13099. [CrossRef] [PubMed]
8. zu Ermgassen, P.S.; Spalding, M.D.; Grizzle, R.E.; Brumbaugh, R.D. Quantifying the loss of a marine ecosystem service: Filtration by the eastern oyster in US estuaries. *Estuaries Coasts* **2013**, *36*, 36–43. [CrossRef]
9. Airoldi, L.; Beck, M.W. Loss, status and trends for coastal marine habitats of Europe. In *Oceanography and Marine Biology*; CRC Press: Boca Raton, FL, USA, 2007; pp. 357–417.
10. Lafferty, K.D.; Harvell, C.D.; Conrad, J.M.; Friedman, C.S.; Kent, M.L.; Kuris, A.M.; Powell, E.N.; Rondeau, D.; Saksida, S.M. Infectious diseases affect marine fisheries and aquaculture economics. *Annu. Rev. Mar. Sci.* **2015**, *7*, 471–496. [CrossRef] [PubMed]
11. Wilberg, M.J.; Livings, M.E.; Barkman, J.S.; Morris, B.T.; Robinson, J.M. Overfishing, disease, habitat loss, and potential extirpation of oysters in upper Chesapeake Bay. *Mar. Ecol. Prog. Ser.* **2011**, *436*, 131–144. [CrossRef]
12. zu Ermgassen, P.S.; Spalding, M.D.; Blake, B.; Coen, L.D.; Dumbauld, B.; Geiger, S.; Grabowski, J.H.; Grizzle, R.; Luckenbach, M.; McGraw, K.; et al. Historical ecology with real numbers: past and present extent and biomass of an imperiled estuarine habitat. *Proc. R. Soc. B Biol. Sci.* **2012**, *279*, 3393–3400. [CrossRef]
13. Baggett, P.L.; Powers, S.P.; Brumbaugh, R.; Coen, L.D.; DeAngelis, B.; Greene, J.; Hancock, B.; Morlock, S. *Oyster Habitat Restoration Monitoring and Assessment Handbook*; The Nature Conservancy: Arlington, VA, USA, 2014; 96p.
14. Brumbaugh, R.D.; Beck, M.W.; Coen, L.D.; Craig, L.; Hicks, P. *A Practitioner's Guide to the Design & Monitoring of Shellfish Restoration Projects: An Ecosystem Services Approach*; The Nature Conservancy: Arlington, VA, USA, 2006.
15. Coen, L.D.; Luckenbach, M.W. Developing success criteria and goals for evaluating oyster reef restoration: ecological function or resource exploitation? *Ecol. Eng.* **2000**, *15*, 323–343. [CrossRef]
16. Oyster Metrics Workgroup (OMW). *Restoration Goals, Quantitative Metrics and Assessment Protocols for Evaluating Success on Restored Oyster Reef Sanctuaries*; Report of the Oyster Metrics Workgroup; Sustainable Fisheries Goal Implementation Team of the NOAA Chesapeake Bay Program: Annapolis, MD, USA, 2011; Available online: http://www.chesapeakebay.net/channel_files/17932/oyster_restoration_success_metrics_final.pdf (accessed on 15 August 2015).
17. Coen, L.D.; Brumbaugh, R.D.; Bushek, D.; Grizzle, R.; Luckenbach, M.W.; Posey, M.H.; Powers, S.P.; Tolley, S.G. Ecosystem services related to oyster restoration. *Mar. Ecol. Prog. Ser.* **2007**, *341*, 303–307. [CrossRef]
18. Grabowski, J.H.; Peterson, C.H. Restoring oyster reefs to recover ecosystem services. *Ecosyst. Eng. Plants Protists* **2007**, *4*, 281–298.
19. Baggett, L.P.; Powers, S.P.; Brumbaugh, R.D.; Coen, L.D.; DeAngelis, B.M.; Greene, J.K.; Hancock, B.T.; Morlock, S.M.; Allen, B.L.; Breitburg, D.L.; et al. Guidelines for evaluating performance of oyster habitat restoration. *Restor. Ecol.* **2015**, *23*, 737–745. [CrossRef]
20. Burrows, F.; Harding, J.M.; Mann, R.; Dame, R.; Coen, L. Chapter 4: Restoration monitoring of oyster reefs. In *Science-Based Restoration Monitoring of Coastal Habitats*; Thayer, G.W., McTigue, T.A., Salz, R.J., Merkey, D.H., Burrows, F.M., Gayaldo, P.F., Eds.; Volume Two: Tools for Monitoring Coastal Habitats; NOAA Coastal Ocean Program Decision Analysis Series No. 23; NOAA National Centers for Coastal Ocean Science: Silver Spring, MD, USA, 2005.
21. Ridge, J.T.; Rodriguez, A.B.; Fodrie, F.J. Evidence of exceptional oyster-reef resilience to fluctuations in sea level. *Ecol. Evol.* **2017**, *7*, 11409–11420. [CrossRef] [PubMed]
22. Ridge, J.T.; Rodriguez, A.B.; Fodrie, F.J.; Lindquist, N.L.; Brodeur, M.C.; Coleman, S.E.; Grabowski, J.H.; Theuerkauf, E.J. Maximizing oyster-reef growth supports green infrastructure with accelerating sea-level rise. *Sci. Rep.* **2015**, *5*, 14785. [CrossRef] [PubMed]

23. Rodriguez, A.B.; Fodrie, F.J.; Ridge, J.T.; Lindquist, N.L.; Theuerkauf, E.J.; Coleman, S.E.; Grabowski, J.H.; Brodeur, M.C.; Gittman, R.K.; Keller, D.A.; et al. Oyster reefs can outpace sea-level rise. *Nat. Clim. Chang.* **2014**, *4*, 493–497. [CrossRef]
24. Grizzle, R.E.; Adams, J.R.; Walters, L.J. Historical changes in intertidal oyster (*Crassostrea virginica*) reefs in a Florida lagoon potentially related to boating activities. *J. Shellfish Res.* **2002**, *21*, 749–756.
25. Grizzle, R.; Ward, K.; Geselbracht, L.; Birch, A. Distribution and Condition of Intertidal Eastern Oyster (Crassostrea virginica) Reefs in Apalachicola Bay Florida Based on High-Resolution Satellite Imagery. *J. Shellfish Res.* **2018**, *37*, 1027–1039. [CrossRef]
26. Twichell, D.C.; Andrews, B.D.; Edmiston, H.L.; Stevenson, W.R. Geophysical Mapping of Oyster Habitats in a Shallow Estuary, Apalachicola Bay, Florida: U.S. Geological Survey Open-File Report 2006-1381. 2007. Available online: http://pubs.usgs.gov/of/2006/1381/ (accessed on 1 May 2019).
27. Walles, B.; Troost, K.; van den Ende, D.; Nieuwhof, S.; Smaal, A.C.; Ysebaert, T. From artificial structures to self-sustaining oyster reefs. *J. Sea Res.* **2016**, *108*, 1–9. [CrossRef]
28. Power, A.; Corley, B.; Atkinson, D.; Walker, R.; Harris, D.; Manley, J.; Johnson, T. A caution against interpreting and quantifying oyster habitat loss from historical surveys. *J. Shellfish Res.* **2010**, *29*, 927–937. [CrossRef]
29. Schill, S.R.; Porter, D.E.; Coen, L.D.; Bushek, D.; Vincent, J. Development of an automated mapping technique for monitoring and managing shellfish distributions. In *NOAA/UNH Cooperative Institute for Coastal and Estuarine Environmental Technology (CICEET)*; University of New Hampshire: Durham, NH, USA, 2006; 91p.
30. Nieuwhof, S.; Herman, P.M.; Dankers, N.; Troost, K.; Van Der Wal, D. Remote sensing of epibenthic shellfish using synthetic aperture radar satellite imagery. *Remote Sens.* **2015**, *7*, 3710–3734. [CrossRef]
31. Garvis, S.K.; Sacks, P.E.; Walters, L.J. Formation, movement, and restoration of dead intertidal oyster reefs in Canaveral National Seashore and Mosquito Lagoon, Florida. *J. Shellfish Res.* **2015**, *34*, 251–258. [CrossRef]
32. ASMFC. *The Importance of Habitat Created by Molluscan Shellfish to Managed Species along the Atlantic Coast of the United States*; Atlantic States Marine Fisheries Commission: Arlington County, VA, USA, 2007.
33. Seavey, J.R.; Pine, W.E.; Frederick, P.; Sturmer, L.; Berrigan, M. Decadal changes in oyster reefs in the Big Bend of Florida's Gulf Coast. *Ecosphere* **2011**, *2*, 1–14. [CrossRef]
34. NOAA Coastal Services Center. Pilot Investigation of Remote Sensing for Intertidal Oyster Mapping in Coastal South Carolina: A Methods Comparison. 2003. Available online: https://coast.noaa.gov/data/digitalcoast/pdf/oyster-mapping.pdf (accessed on 16 September 2018).
35. South Carolina Department of Natural Resources (SCDNR), Marine Resources Division. *Final Report for South Carolina's 2004-05 Intertidal Oyster Survey and Related Reef Restoration/Enhancement Program*; NOAA Award No. NA04NMF4630309; South Carolina Department of Natural Resources (SCDNR), Marine Resources Division: Columbia, SC, USA, 2008; Available online: http://www.oyster-restoration.org/wp-content/uploads/2012/06/Final-Report-for-Oyster-Survey-and-Recovery-Phase-II-with-appendices.pdf (accessed on 16 September 2018).
36. Guillen, G.; Mokrech, M. *Mapping Shallow Reefs Using Low-Cost Scanning Sonar and Drone Photography Systems*; EIH Final Report # 18-001; Environmental Institute of Houston: Houston, TX, USA, 2018. Available online: https://www.sciencebase.gov/catalog/item/5bf82b0fe4b045bfcae2eaae (accessed on 1 May 2019).
37. Johnston, D.W. Unoccupied Aircraft Systems in Marine Science and Conservation. *Ann. Rev. Mar. Sci.* **2019**, *11*, 439–463. [CrossRef] [PubMed]
38. Joyce, K.E.; Duce, S.; Leahy, S.M.; Leon, J.; Maier, S.W. Principles and practice of acquiring drone-based image data in marine environments. *Mar. Freshw. Res.* **2018**, *70*, 952–963. [CrossRef]
39. Klemas, V.V. Coastal and environmental remote sensing from unmanned aerial vehicles: An overview. *J. Coast. Res.* **2015**, *31*, 1260–1267. [CrossRef]
40. Mancini, F.; Dubbini, M.; Gattelli, M.; Stecchi, F.; Fabbri, S.; Gabbianelli, G. Using unmanned aerial vehicles (UAV) for high-resolution reconstruction of topography: The structure from motion approach on coastal environments. *Remote Sens.* **2013**, *5*, 6880–6898. [CrossRef]
41. Seymour, A.C.; Ridge, J.T.; Rodriguez, A.B.; Newton, E.; Dale, J.; Johnston, D.W. Deploying fixed wing Unoccupied Aerial Systems (UAS) for coastal morphology assessment and management. *J. Coast. Res.* **2017**, *34*, 704–717. [CrossRef]
42. R Core Team. *R: A Language and Environment for Statistical Computing*; R Foundation for Statistical Computing: Vienna, Austria, 2013.

43. Le Bris, A.; Rosa, P.; Lerouxel, A.; Cognie, B.; Gernez, P.; Launeau, P.; Robin, M.; Barillé, L. Hyperspectral remote sensing of wild oyster reefs. *Estuar. Coast. Shelf Sci.* **2016**, *172*, 1–12. [CrossRef]
44. O'Keife, K.; Arnold, W.; Reed, D. Tampa Bay oyster bar mapping and assessment. In *Final Report to Tampa Bay Estuary Program*; Technical Publication: Maharashtra, India, 2006.
45. Casella, E.; Collin, A.; Harris, D.; Ferse, S.; Bejarano, S.; Parravicini, V.; Hench, J.L.; Rovere, A. Mapping coral reefs using consumer-grade drones and structure from motion photogrammetry techniques. *Coral Reefs* **2017**, *36*, 269–275. [CrossRef]
46. Sturdivant, E.; Lentz, E.; Thieler, E.R.; Farris, A.; Weber, K.; Remsen, D.; Miner, S.; Henderson, R. UAS-SfM for coastal research: Geomorphic feature extraction and land cover classification from high-resolution elevation and optical imagery. *Remote Sens.* **2017**, *9*, 1020. [CrossRef]
47. Yaney-Keller, A.; Tomillo, P.S.; Marshall, J.M.; Paladino, F.V. Using Unmanned Aerial Systems (UAS) to assay mangrove estuaries on the Pacific coast of Costa Rica. *PLoS ONE* **2019**, *14*, e0217310. [CrossRef]
48. Burns, J.H.R.; Delparte, D.; Gates, R.D.; Takabayashi, M. Integrating structure-from-motion photogrammetry with geospatial software as a novel technique for quantifying 3D ecological characteristics of coral reefs. *Peer J.* **2015**, *3*, e1077. [CrossRef] [PubMed]